

M. TRYBUŁA\*<sup>‡</sup>, N. JAKSE\*\*, W. GAŚSIOR\*, A. PASTUREL\*\*

## THERMODYNAMICS AND CONCENTRATION FLUCTUATIONS OF LIQUID Al-Cu AND Al-Zn ALLOYS

### TERMODYNAMIKA I FLUKTUACJE STĘŻENIA CIEKŁYCH STOPÓW Al-Cu ORAZ Al-Zn

Thermodynamic properties of liquid Al-Cu and Al-Zn alloys are investigated using the free volume model. We also analyse local atomic arrangements and concentration fluctuations in both liquid binary alloys from the determination of the Warren-Cowley short-range order. For liquid Al-Cu alloys, our findings indicate a strong preference for heteroatomic nearest-neighbors bonds on the Cu-rich side and weaker ones in the Al-rich part while for the liquid Al-Zn alloy, a tendency to the phase separation is observed. Basing on Darken's thermodynamic relationship, diffusivity has been examined for both liquid alloys.

*Keywords:* Al-Cu alloys, Al-Zn alloys, CSRO parameter, free volume model, diffusivity

W oparciu o model swobodnej objętości zostały zbadane właściwości termodynamiczne ciekłych stopów Al-Cu i Al-Zn oraz lokalne środowisko atomów w celu obliczenia parametru bliskiego zasięgu Warren-Cowleya. W ciekłych stopach Al-Cu zaobserwowano silną tendencję do tworzenia wiązań hetero-atomowych w obszarze bogatym w Cu, natomiast w obszarze stężeń bogatych w Al znacznie słabszą. W przypadku ciekłych stopów Al-Zn obliczenia wskazują na tendencję do segregacji atomów. Dyfuzja w dyskutowanych stopach została przeanalizowana w oparciu o termodynamiczną definicję podaną przez Darkena.

### 1. Introduction

Different theoretical models were proposed to describe the concentration dependence of thermodynamic properties of liquid binary systems. Investigations towards the estimation of thermodynamic properties using the free volume theory for dilute liquid binary alloys were early done by Shimoji and Niwa [1]. Later, Tanaka and Gokcen [2-4] extended them to concentrated metallic solutions where the short-range order in the local configuration of atoms should be considered. This local environment can be studied from the Bathia-Thornton theory [5-7] using two microscopic functions: concentration fluctuation function and chemical short-range order parameter ( $\alpha_1$ ) [8-9]. These properties are useful for describing and understanding the mechanism of compound formation or phase segregation in liquid alloys. Moreover they showed that the knowledge which comes from density and mixing enthalpy is sufficient to model the excess thermodynamic functions (entropy and Gibbs energy) at each composition of the system. The main advantage of this model is that we can evaluate the non-configurational entropy – namely the vibrational contribution, which is usually neglected [10-15].

The investigated liquid binary alloys: Al-Zn and Al-Cu display positive and negative deviation from Raoult's law,

respectively. The Al-Cu system is characterized by a large amount of intermetallic phases in the solid state in comparison to Al-Zn for which miscibility gap occurs. Then, the first objective of our work is to understand why two Al-based alloys exhibit a different tendency for chemical bonding without using the explicit presence of any "associate form" in the liquid state, as done in the compound formation model [15]. At the beginning of our study, the mixing thermodynamic properties: entropy and Gibbs energy for liquid Al-Cu alloys at 1370K and for liquid Al-Zn at 1000K are investigated. Secondly, the Bathia-Thornton [5-7] formalism was used to analyse microscopic functions and diffusivity in both liquid binary alloys. Our choice of these alloys was influenced by the availability of all the required thermodynamic and density (mixing volume) properties.

### 2. Theory

#### 2.1. The free volume model [1-4]

Within the free atom theory, each atom is placed in a restricted region in a cell composed of the nearest neighbour atoms. Different configurations mostly depending upon the number of atoms present in the restricted region (free volume)

\* INSTITUTE OF METALLURGY AND MATERIALS SCIENCE POLISH ACADEMY OF SCIENCES, KRAKOW, POLAND

\*\* LABORATOIRE DE SCIENCE ET INGENIERIE DES MATERIAUX ET PROCEDES, UMR-CNRS-INPG-UFJ 5266, PHELMA-GRENOBLE-INP, SAINT-MARTIN-D'HERES CEDEX, FRANCE

<sup>‡</sup> Corresponding author: m.trybula@imim.pl

are expressed by a partition function given by the formula well described in Ref. [11].

Basing on a relationship between phenomenological and statistical thermodynamics, the thermodynamic functions can be expressed as following.

**2.1.a Enthalpy term**

The enthalpy of mixing defined in Eq. (1) is crucial for the estimation of the exchange energy parameter *W* and the combinatorial factor *P*. It is written as follows:

$$\Delta H_{mix} = \frac{2x(1-x)W}{P+1}; \tag{1}$$

Where *P* is defined by:

$$P = \left[ 1 + 4x(1-x) \left[ \exp\left(\frac{W}{RT}\right) - 1 \right] \right]^{1/2} \tag{2}$$

where *x* – mole fraction of alloy component, *R* – gas constant, *T* – absolute temperature.

Depending on the sign of mixing enthalpy, the parameter *P* is computed as follows:

- a) For positive mixing enthalpy, *P* is set to unity, due to the assumption of a nearly random configuration of atoms in a cell
- b) For negative mixing enthalpy, *P* is expanded in Taylor series of the function form:

$$(1+y)^{1/2} = 1 + \frac{y}{2} - \frac{y^2}{8} + \frac{y^3}{16} - \dots \tag{3}$$

where:  $y = 4x(1-x) \left[ \exp\left(\frac{W}{RT}\right) - 1 \right]$ .

After application of the above mentioned formula, the negative mixing enthalpy can be expressed as follows:

$$\Delta H_{mix} = x(1-x)W \left( 1 - x(1-x) \left[ \exp\left(\frac{W}{RT}\right) - 1 \right] + 2x(1-x) \left[ \exp\left(\frac{W}{RT}\right) - 1 \right]^2 - 5x(1-x) \left[ \exp\left(\frac{W}{RT}\right) - 1 \right]^3 + \dots \right) \tag{4}$$

**2.1.b Entropy terms**

Excess entropy of binary systems consists of two parts: the first arises from atomic configurations ( $\Delta S_{conf}$ ) while the second describes atomic vibrations ( $\Delta S_{vib}$ ).

The first part of the excess entropy related to atomic configurations is given by:

$$\Delta S_{conf} = \frac{2x(1-x)W}{P+1} - R \cdot (1-x) \cdot \ln\left(\frac{P+1-2x}{(1-x) \cdot (P+1)}\right) - R \cdot x \cdot \ln\left(\frac{P+2x-1}{x \cdot (P+1)}\right) \tag{5}$$

It is obtained basing on a first approximation of the regular solution model [16]. When the mixing enthalpy has positive values, the excess configurational entropy equals to zero due to the assumption of a nearly random atoms configuration of the considered alloy.

The second contribution to the excess entropy arising from atomic vibrations can be derived from the formulae (6):

$$\Delta S_{vib} = \frac{3}{2} \cdot R \cdot \left[ 2 \cdot (1-x) \cdot \ln\left(\frac{L_{AA}}{L_A}\right) + 2 \cdot x \cdot \ln\left(\frac{L_{BB}}{L_B}\right) + (1-x) \cdot \ln\left(\frac{U_A}{U_{AA}}\right) + x \cdot \ln\left(\frac{U_B}{U_{BB}}\right) \right] \tag{6}$$

The excess vibrational entropy is a function of bond lengths, and bond energies of pure components as well as in the mixture [2-4].

The mean bond lengths of A and B atoms in pure liquids ( $L_{AA}$ ,  $L_{BB}$ ) and in the binary alloy ( $L_A$ ,  $L_B$ ) in Eq. (6) are given:

$$L_{AA} = \frac{1}{2} \left( \frac{\sqrt{2} V_{AA}^{pure}}{N} \right)^{1/3}; \quad L_{BB} = \frac{1}{2} \left( \frac{\sqrt{2} V_{BB}^{pure}}{N} \right)^{1/3} \\ L_A = \frac{1}{2} \left( \frac{\sqrt{2} V_A}{N} \right)^{1/3}; \quad L_B = \frac{1}{2} \left( \frac{\sqrt{2} V_B}{N} \right)^{1/3} \tag{7}$$

These relations are derived by assuming the half of the nearest-neighbour distance between atoms and it can be computed from molar volumes of elements in pure liquids ( $V_A^{pure}$ ,  $V_B^{pure}$ ) and in the binary alloy ( $V_A$ ,  $V_B$ ).

The bond energy – depth of the potential energy curve of pure components A and B,  $U_X$  [J/mol] in eq. (6), are computed applying the harmonic approximation, given as:

$$U_{XX} = -685 \cdot \beta_X^2 \cdot T_{m,X} \tag{8}$$

$T_{m,X}$  is the temperature at the melting point of pure components A and B,  $\beta_X$  is a correction factor. This coefficient can be understood as an anharmonic addition to the harmonic vibration of atoms. It can depend on many different physical properties. One formula brings together surface tension ( $\sigma_{X,m}$ ), molar volume ( $V_{m,X}$ ), temperature ( $T_{m,X}$ ) and packing factor ( $\eta_{X,m}$ ) at the melting point of pure metals (eq. (8)) [17], which originally was applied by Tanaka and Gokcen [2-4,17].

$$\beta_X = - \frac{1.1 \cdot 10^3 V_{X,m}^{1/3}}{1.97 \eta_{X,m}^{1/3} - 1} \left( \frac{\sigma_{X,m}}{R T_{m,X}} \right) \tag{9}$$

Another formula relates the beta parameter to the velocity of sound and the melting temperature of pure elements [17]. However, studies performed for many liquid metallic solutions indicate that Eq. (9) is sufficient for computing the excess vibrational entropy.

The bond energy of atoms in binary alloy ( $U_A$ ,  $U_B$ ) is computed from equation (10) [2-4]:

$$U_A = \left( 1 - \frac{2x}{P+1} \right) \cdot U_{AA} + \left( \frac{2x}{P+1} \right) \cdot \left( W + \frac{U_{AA} + U_{BB}}{2} \right); \\ U_B = \left( 1 - \frac{2(1-x)}{P+1} \right) \cdot U_{BB} + \left( \frac{2(1-x)}{P+1} \right) \cdot \left( W + \frac{U_{AA} + U_{BB}}{2} \right) \tag{10}$$

where:  $U_A$  depends on the fraction of A atoms among the nearest-neighbours of A atoms in the alloy and the fraction of B atoms in the surroundings of A atoms, similarly for  $U_B$ . The second term in both expressions represents the potential energy of unlike atoms  $U_{AB}$ . The difficulty in obtaining  $U_{AB}$  from physical properties of liquid binary alloy leads to approximate the value  $U_{AB}$  from values of  $U_{AA}$ ,  $U_{BB}$  and *W*:

$$U_{AB} = W + \left( \frac{U_{AA} + U_{BB}}{2} \right) \tag{11}$$

## 2.2. Microscopic functions

The concentration fluctuation function  $S_{CC}(0)$  is an important contribution to understand the structure and the binding of atoms at the microscopic level [6]. It is related to ordering effects in binary liquid alloys [18-19]. This microscopic function is thermodynamically associated to the mixing Gibbs energy,  $G_M = G_M^{xs} + RT \sum_i C_i \ln C_i$ , and the activity of pure components ( $a_A$  and  $a_B$ ) [6]. It can be written in the following form:

$$S_{CC}(0) = RT \left( \frac{\partial^2 G_M}{\partial C_A^2} \right)^{-1} = C_B a_A \left( \frac{\partial a_A}{\partial C_A} \right)^{-1} = C_A a_B \left( \frac{\partial a_B}{\partial C_B} \right)^{-1} \quad (12)$$

For an ideal mixing, the energy parameter  $W$  in eq. (1) equals zero and the concentration-concentration fluctuation function ( $S_{CC}(0, id)$ ) is given:

$$S_{CC}(0, id) = C(1 - C)(C = C_B) \quad (13)$$

Deviation of  $S_{CC}(0)$  from the ideal mixing –  $S_{CC}(0, id)$  is an important factor for the description of the nature of atomic interactions in the mixture. The presence of a chemical ordering is exhibited by the inequality  $S_{CC}(0) < S_{CC}(0, id)$ , while the phase segregation leads to the inequality  $S_{CC}(0) > S_{CC}(0, id)$  [18-19]. To quantify ordering or segregation effects in the melt, the Warren-Cowley short-range order parameter ( $\alpha_1$ ) [8-9] has been computed. It gives an insight into the local arrangement of atoms in the molten systems. This parameter is related to  $S_{CC}(0)$  by the relation:

$$\alpha_1 = \frac{A - 1}{A(Z - 1) + 1} \quad (14)$$

$Z$  is the coordination number taken as 10 [10] and  $A = \frac{S_{CC}(0)}{S_{CC}(0, id)}$ . For the equiatomic composition,  $\alpha_1$  is found to be within the range of  $(-1, 1)$ , the value -1 means a complete ordering in the AB alloy and suggests a tendency for the compound formation, whereas,  $\alpha_1 = 1$  indicates the segregation of constituent elements in the AB melt [20].

## 2.3. Diffusivity

The knowledge of dynamic properties is required for understanding and explaining at the microscopic scale the process of mixing between the two atomic species of a binary liquid alloy.

Based on Darken's thermodynamic equation [21], the relation between diffusion and  $S_{CC}(0)$  can be written as:

$$\frac{D_M}{D_{id}} = \frac{S_{CC}(0, id)}{S_{CC}(0)} \quad (15)$$

where  $D_M$  is the mutual diffusion coefficient and  $D_{id}$  is the intrinsic diffusion coefficient for ideal mixture [22]. It is given as follows:

$$D_{id} = C_A D_B + C_B D_A \quad (16)$$

$D_A, D_B$  define the self-diffusion coefficients of A and B constituents in the alloy. For a system having a tendency to compound formation, both inequalities, ( $S_{CC}(0) > S_{CC}(0, id)$ ) and  $D_M > D_{id}$  are satisfied. Note that the pronounced peak in the concentration dependence of  $D_M/D_{id}$  is often related to the formation of the most probable associates in the liquid phase [23-24].

## 3. Modelling

A program for computing mixing thermodynamic properties using the free volume model theory [2-4] was written by one of co-authors and least-squares fitting procedure was used to determine the exchange energy parameter,  $W$ , in Eq. (4). The assessment of  $W$  allows to compute the combinatorial factor,  $P$ . They are necessary for the evaluation of the excess entropies as well as the Gibbs energy, finally.

For relative simplicity, the modeled mixing Gibbs energy,  $G_m$ , is expressed by means of Redlich-Kister polynomial (RK) reported in [25]. Its mathematical representation is as follows:

$$G_m = G^{xc} + RT((1 - C_B) \ln(1 - C_B) + C_B \ln C_B) \quad (17)$$

$$G^{xc} = L^0 + L^1(C_A - C_B) + L^2(C_A - C_B)^2 + \dots + L^n(C_A - C_B)^n \quad (18)$$

Where:  $G^{xc}$  is the excess Gibbs energy and  $L^i$  ( $i=0,1,2,\dots,n$ ) are thermodynamic parameters.

The least-squares fitting procedure for the modeled data was applied to assess the  $L^i$  constants in Eq. (18). Then, the obtained thermodynamic parameters set, inserted in Table 1, were used to determine  $S_{CC}(0)$  from Eq.12 and  $\alpha_1$  parameter from Eq. 14.

For experimental data, let us mention that we have also used the RK representation to express the Gibbs energy. RK parameters used for its determination are collected in Table 1 for liquid Al-Cu [26] and Al-Zn [27] alloys. Other parameters like  $\beta$  parameter, melting temperature and volumes of pure elements ( $V_m^{pure}$ ) required to compute the mixing functions are taken from ref. [17] and collected in Table 2.

TABLE 1

Redlich-Kister parameters from experiment and free volume model of liquid Al-Cu and Al-Zn alloys

System		$L^0(T)$	$L^1(T)$	$L^2(T)$	$L^3(T)$
experiment	Al-Cu <sup>[26]</sup>	-66622+8.1*T	46800-90.8*T+10*T*lnT	-2812	-
	Al-Zn <sup>[27]</sup>	10466.3-3.393*T	-	-	-
FVM	Al-Cu	-24207.2-17.62*T	10308.5+7.501*T+1.036*lnT	-2240.8-1.63*T	-5770.5
	Al-Zn	3949.7+3.92*T	-	-	-

TABLE 2

$\beta$  parameters, temperature at melting point and molar volume of pure components (Al, Zn and Cu)<sup>[17]</sup>

element	$\beta$	$T_m$ [K]	$V_m^{pure}$ [cm <sup>3</sup> ]
Al	0.48	933.35	11.3
Zn	0.54	692.62	9.94
Cu	0.46	1233.65	7.94

Densities of liquid binary Al-Cu and Al-Zn alloys were taken from [28] and [29], respectively and were used to compute the molar volume of mixture ( $V_m$ ) and evaluate partial molar volumes ( $V_A$ ,  $V_B$ ) by applying Gibbs-Duhem relation as follows:

$$V_m = C_A V_A + C_B V_B \quad (19)$$

#### 4. Results and Discussion:

##### *Thermodynamic properties of liquid Al-Cu and Al-Zn alloys*

The mixing thermodynamic properties: mixing enthalpy, entropy and Gibbs energy of liquid binary Al-Cu at 1373K and Al-Zn at 1000K alloys have been analysed in the framework of the free volume model (FVM) [2-4]. They are compared to available experimental data taken from [26] for liquid Al-Cu and [27] for Al-Zn.

The computed bond energies and bond lengths of each component in the melt using Eqs. (7-8, 10-11) are listed in Table 3 as well as the computed excess entropies and Gibbs energies of both liquid alloys. Significant variation of bond lengths of AlAl and CuCu pairs in Al-Cu alloys are obtained in comparison to relatively constant bond lengths of AlAl and ZnZn pairs in liquid Al-Zn alloys.

TABLE 3

Concentration, enthalpy of mixing, P combinatorial factor, bond lengths and bond energies of each alloy component ( $L_i$ ,  $U_i$ ), the excess entropy and Gibbs energy computed using FVM formalism[2-4]: a) Al-Cu alloys at 1373K and b) Al-Zn alloys at 1000K

a)	Al-Cu at 1373K							
$C_{Cu}$	$\Delta H_m$ [kJ/mol]	P	$L_{Al}$ [10 <sup>-8</sup> cm]	$L_{Cu}$ [10 <sup>-8</sup> cm]	$U_{Al}$ [kJ/mol]	$U_{Cu}$ [kJ/mol]	$\Delta S^{xc}$ [J/molK]	$\Delta G^{xc}$ [kJ/mol]
0.0	0	-	1.46	-	-147.305	-	0	0
0.2	-7.646	0.617	1.49	1.12	-162.955	-210.436	-1.87	-5.071
0.3	-11.307	0.431	1.48	1.18	-173.786	-210.159	-2.52	-7.843
0.4	-14.428	0.255	1.45	1.22	-187.047	-209.098	-3.15	-10.099
0.5	-16.655	0.141	1.41	1.25	-202.205	-208.290	-3.35	-12.057
0.6	-17.603	0.227	1.40	1.27	-215.392	-209.855	-3.26	-13.117
0.7	-16.862	0.406	1.38	1.27	-228.039	-210.147	-3.19	-12.480
0.8	-13.996	0.601	1.37	1.28	-241.900	-207.910	-2.33	-10.795
1.0	0	-	-	1.28	-	-196.568	0	0
b)	Al-Zn at 1000K							
$C_{Zn}$	$\Delta H_m$ [kJ/mol]	P	$L_{Al}$ [10 <sup>-8</sup> cm]	$L_{Zn}$ [10 <sup>-8</sup> cm]	$U_{Al}$ [kJ/mol]	$U_{Zn}$ [kJ/mol]	$\Delta S^{xc}$ [J/molK]	$\Delta G^{xc}$ [kJ/mol]
0.0	0	-	1.38	-	-147.305	-	0	0
0.1	0.942	1.00	1.39	1.40	-145.850	-133.065	0.25	0.688
0.2	1.675	1.00	1.39	1.40	-144.362	-133.670	0.44	1.230
0.3	2.197	1.00	1.39	1.40	-142.874	-134.276	0.57	1.625
0.4	2.512	1.00	1.39	1.40	-141.386	-134.881	0.64	1.871
0.5	2.617	1.00	1.39	1.40	-139.898	-135.487	0.65	1.965
0.6	2.511	1.00	1.39	1.41	-138.410	-136.092	0.61	1.903
0.7	2.197	1.00	1.39	1.41	-136.923	-136.698	0.52	1.680
0.8	1.674	1.00	1.39	1.41	-135.435	-137.303	0.38	1.292
0.9	0.941	1.00	1.39	1.41	-133.670	-137.910	0.21	0.733
1.0	0	-	-	1.39	-	-138.514	0	0

The comparative studies presented in Figure 1 show that liquid Al-Cu alloys display negative deviation from Raoult's law.

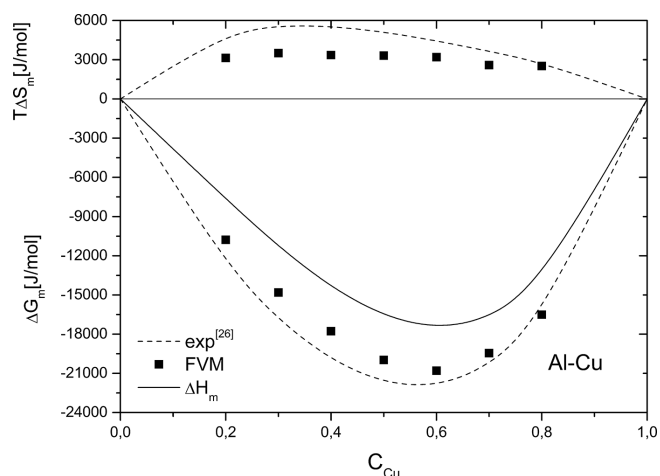


Fig. 1. Concentration dependencies of the mixing thermodynamic functions: entropy and Gibbs energy ( $T\Delta S$  and  $\Delta G$ ) for set of RK parameters [26] – dashed line and FVM data – squares but mixing enthalpy – solid line of the liquid Al-Cu at 1373K

Mixing enthalpy and Gibbs energy have negative values in contrast to the mixing entropy, which is positive but smaller than for ideal mixing. Bond lengths analysis of each atom pairs in the Al-Cu melts lead to the same trend since they are shorter in the melt than for pure liquid states. The concentration dependencies of computed mixing thermodynamic functions display an asymmetrical shape characterized by a minimum shifted toward copper rich alloys, in fair agreement with experimental data. However, we can note that modelled data of the mixing entropy underestimate slightly the experimental ones in the Al-rich side.

Very weak deviations between theory and experiment [27] appear for liquid binary Al-Zn alloys displaying positive deviation from Raoult's law. Concentration dependencies of each investigated mixing thermodynamic properties are presented in Figure 2.

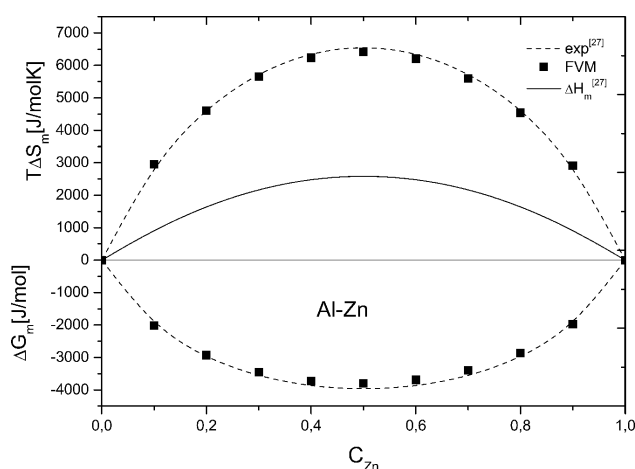


Fig. 2. Concentration dependencies of the mixing thermodynamic functions: entropy and Gibbs energy ( $T\Delta S$  and  $\Delta G$ ) for set of RK parameters [27] – dashed line and FVM data – squares but mixing enthalpy – solid line of the liquid Al-Zn at 1000K

These thermodynamic properties have maxima/minima located at the equiatomic composition as for a regular solution.

*Microscopic functions: the concentration-concentration function and the short-range order parameter*

The ordering tendency of liquid Al-Cu alloys at 1373K and the phase segregation exhibiting in liquid Al-Zn alloys at 1000K have been analysed through the concentration fluctuation function in the long wavelength limit,  $S_{CC}(0)$  [6]. The experimental concentration fluctuation function has been computed from the known mixing Gibbs energy, given by Eq. (17), using Eq. (12). Further, It is used to analyse the local atomic arrangements expressed by means of Warren-Cowley short-range order parameter [8,9] formulated by Eq. (14).

Computed  $S_{CC}(0)$  and  $\alpha_1$  of liquid Al-Cu alloys at 1373K are plotted in Figure 3 as a function of copper concentration. Figure 3 includes also those obtained from measurement [26].

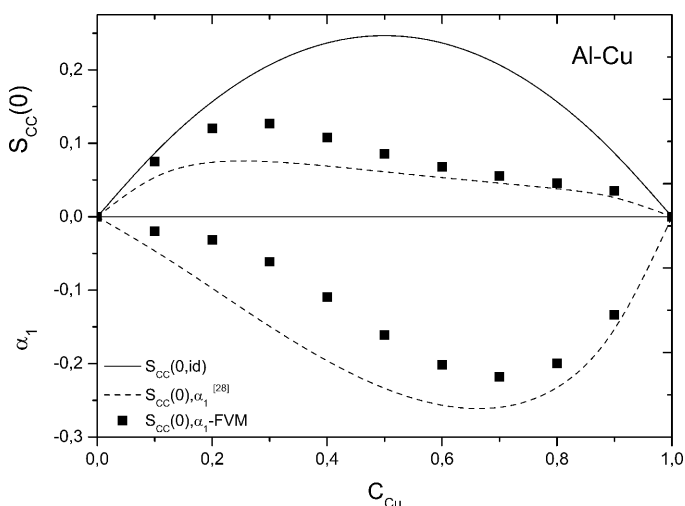


Fig. 3. Concentration-concentration fluctuation function ( $S_{CC}(0)$ ) and chemical short-range order parameter,  $\alpha_1$ , of the liquid Al-Cu alloys at 1373K: RK parameters [26] – dashed line but FVM data – squares and ideal mixing function ( $S_{CC}(0, id)$ ) – solid line

These values clearly show a minimum in the range of copper-rich alloys where intermetallic phases occur. It can be noticed that the modelled and experimental concentration fluctuation functions, have lower values than  $S_{CC}(0, id)$ , indicating a strong tendency to form heteroatomic bonds. Both modelled and experimental Warren-Cowley short-range order parameters determined from Eq.(14) also confirm this tendency to the compound formation of liquid Al-Cu alloys in the region of intermetallic phases. The experimental asymmetrical shape of  $\alpha_1$  curve with respect to the copper concentration is well reproduced by the FVM model as well as high negative values in the Cu-rich side. However, significant deviations between modelled and experimental data can be noticed in the aluminium rich region where the free volume model underestimates ordering effects obtained experimentally, like for the excess entropy.

However, let us mention that we obtain the same behaviour for liquid AlCu and AlLi alloys using the compound formation model [30, 31] emphasizing the difficulty for simple phenomenological thermodynamic models to describe ordering phenomena quantitatively.

The concentration fluctuation function  $S_{CC}(0)$  for liquid Al-Zn alloys at 1000K in function of the zinc concentration is drawn in Figure 4.

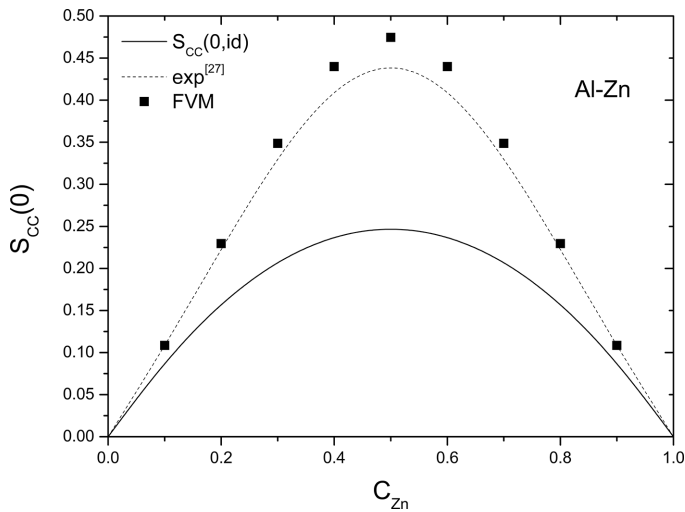


Fig. 4. Concentration-concentration fluctuation function ( $S_{CC}(0)$ ) and chemical short-range order parameter,  $\alpha_1$ , of the liquid Al-Zn alloys at 1000K: RK parameters [27] – dashed line but FVM data – squares and ideal mixing function ( $S_{CC}(0, id)$ ) – solid line

It can be noticed that  $S_{CC}(0)$  has higher values than  $S_{CC}(0, id)$  for the ideal mixing, indicating a tendency to the phase segregation. Maxima of experimental and modelled  $S_{CC}(0)$  are located at the equiatomic concentration ( $C_{Zn} = 0.5$ ). The computed chemical short-range order parameters ( $\alpha_1$ ) using Eq. (14) are listed in Table 4.

TABLE 4

The computed chemical short-range order parameter ( $\alpha_1$ ) for RK parameters from [27] and in the framework of FVM for the liquid Al-Zn alloys at 1000K

$C_{Zn}$	$\alpha_1^{[27]}$	$\alpha_1$
0	0	0
0.1	0.0162	0.0173
0.2	0.0292	0.0312
0.3	0.0386	0.0414
0.4	0.0444	0.0476
0.5	0.0463	0.0496
0.6	0.0444	0.0476
0.7	0.0386	0.0414
0.8	0.0292	0.0312
0.9	0.0162	0.0173
1	0	0

Both CSRO parameters have positive values characterized by a maximum located at the equiatomic concentration. Similar results are obtained by authors of this work using the Quasi-Lattice Theory and molecular dynamics simulations [33]. Our results are also consistent with those computed for another set of RK parameters [29] and data modelled using the Quasi-Lattice theory as obtained by Odusote [34].

### Diffusivity

We have investigated the diffusivity of liquid Al-Cu and Al-Zn alloys, respectively using eq. (15). Concentration dependencies of  $D_m/D_{id}$  are shown in Figure 5 and 6 for liquid Al-Cu and Al-Zn alloys respectively.

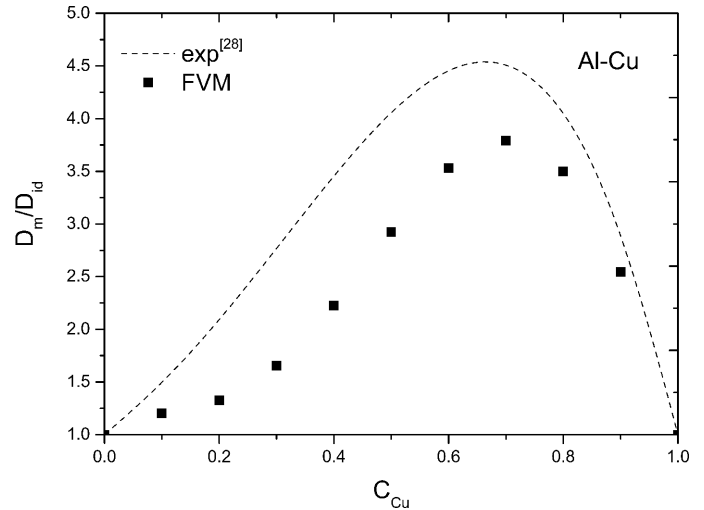


Fig. 5. Diffusivity ratio of the liquid Al-Cu alloys at 1000K: computed for RK parameters listed in Table 1 [26] – dashed line and FVM data – squares

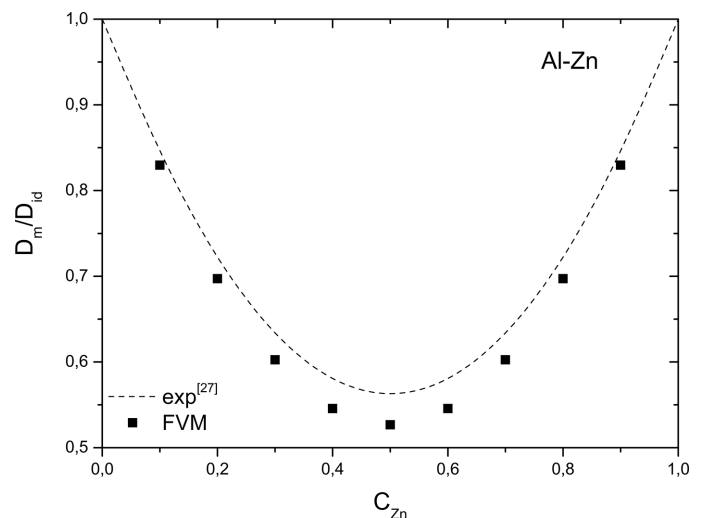


Fig. 6. Diffusivity ratio of the liquid Al-Zn alloys at 1000K: computed for RK parameters listed in Table 1 [27] – dashed line and FVM data – squares

The observed tendencies can be related to changes observed for the short-range order parameter,  $\alpha_1$ .

In the case of liquid Al-Cu alloys, the discrepancy of  $D_m/D_{id}$  between the FVM data and experimental ones is around ten percent and both maxima occur at the vicinity of the gamma intermetallic phase.

For liquid Al-Zn alloys, a better correlation is obtained. A very small mismatch of  $D_m/D_{id}$  between computed – FVM data and experimental ones is noticed at the equiatomic composition. This trend is also obtained using the Quasi-Lattice theory and classical molecular dynamics method presented in [30].

It is important to stress that investigated dynamic properties of liquid binaries confirm the tendency to the compound formation of liquid Al-Cu alloys and to the phase segregation in liquid Al-Zn alloys.

## 5. Conclusions

The estimated thermodynamic functions: mixing entropy and Gibbs energy based on the free volume model are in good agreement with experimental data for Al-Zn alloys. For liquid Al-Cu alloys, the experimental asymmetrical shape of mixing functions: Gibbs energy, enthalpy, excess entropy is well reproduced by the FVM data, characterized by maxima around 0.6 copper mole fraction. We obtain the same trend for the  $S_{CC}(0)$  function and the  $\alpha_1$  parameter. However, we note that the FVM underestimates ordering effects, especially in the Al-rich region. We should underline that we obtain a similar trend for liquid Al-Cu [30] and Al-Li [31] alloys computed within compound formation model, emphasizing the difficulty to reproduce ordering effects quantitatively, using simple thermodynamic models.

## Acknowledgements

Financial support for research was provided by European Union in the framework of European Social Fund, project number POKL.04.01.01-00-004/10.

## REFERENCES

- [1] M. Shimoji, K. Niwa, *Acta Metall.* **5**, 496 (1957).
- [2] T. Tanaka, N.A. Gokcen, Z. Morita, *Z. Metallkd.* **81**, 349-353 (1990).
- [3] T. Tanaka, N.A. Gokcen, Z. Morita, *Z. Metallkd.* **81**, 49-54 (1990).
- [4] T. Tanaka, N.A. Gokcen, Z. Morita, T. Iida, *Z. Metallkd.* **84**, 192-200 (1993).
- [5] A.B. Bhatia, W.H. Hargrove, *Lett. Al Nuovo Cim. Ser. 2*, **8**, 1025 (1973).
- [6] A.B. Bhatia, W. Hargrove, *Phys. Rev. B* **10**, 3186 (1974).
- [7] A.B. Bhatia, W.H. Hargrove, N.H. March, *J. Phys. C Solid State Phys.* **6**, 621 (1973).
- [8] J.M. Cowley, *Phys. Rev.* **77**, 667 (1950).
- [9] E. Warren, B. X-ray Diffraction. Reading MA : Addison-Wesley, 1969.
- [10] E.A. Guggenheim, *Mixtures*. Oxford: University Press, 1952.
- [11] C.H.P. Lupis, J.F. Elliot, *Acta Metall.* **15**, 265-276 (1967).
- [12] A.B. Bhatia, R.N. Singh, *Phys. Chem. Liq.* **11**, 285 (1982).
- [13] A.B. Bhatia, R.N. Singh, *Phys. Chem. Liq.* **11**, 343 (1982).
- [14] A.B. Bhatia, R.N. Singh, *Phys. Chem. Liq.* **13**, 177 (1984).
- [15] R. Novakovic, E. Ricci, M.L. Muolo, D. Giuranno, A. Passerone, *Intermetallics* **11**, 1301 (2003).
- [16] N.A. Gokcen, *Statistical Thermodynamics of Alloys*. New York: Plenum Press, 101-104 (1986).
- [17] T. Iida, R.I.L. Guthrie, *The Physical Properties of Liquid Metals*. Oxford: Clarendon Press **6**, 7, 97-100, 125-131 (1988).
- [18] R.N. Singh, *Can. J. Phys.* **65**, 309 (1987).
- [19] R.N. Singh, *Phys. Chem. Liq.* **25**, 251 (1993).
- [20] R.N. Singh, F. Sommer, *Reports Prog. Phys.* **60**, 57 (1997).
- [21] L. Darken, *Trans. Met. Soc. Aime* **175**, 184 (1948).
- [22] R.N. Singh, F. Sommer, *Phys. Chem. Liq.* **36**, 17 (1998).
- [23] R. Novakovic, M. Muolo, A. Passerone, *Surf. Sci.* **549**, 281 (2004).
- [24] R. Novakovic, E. Ricci, D. Giuranno, A. Passerone, *Surf. Sci.* **576**, 175 (2005).
- [25] O. Redlich, A.T. Kister, *Ind. Eng. Chem.* **40**, 345 (1948).
- [26] V.T. Witusiewicz, U. Hecht, S.G. Fries, S. Rex, *J. Alloy Comp.* **385**, 133-143 (2004).
- [27] S-L. Chen, Y.A. Chang, *Calphad* **17**, 113-124 (1993).
- [28] J. Brillo, I. Egry, J. Westphal, *Int. J. Mat. Res.* **99**, 2 (2008).
- [29] E. Gebhardt, M. Becker, S. Dorner, *Z. Metallkde.* 1954.
- [30] M. Trybula, N. Jakse, L. Hennet, W. Gasior, A. Pasturel (unpublished).
- [31] M. Trybula, T. Gancarz, W. Gasior, A. Pasturel, *Metall. Mater. Trans. A* **45**, 5517-5530 (2014).
- [32] L.C. Prasad, A. Mikula, *Physica B* **373**, 142-149 (2006).
- [33] M. Trybula, N. Jakse, W. Gasior, A. Pasturel *J. Chem. Phys.* **141**, 1-9 (2014).
- [34] Y.A. Odusote, L.A. Hussain, O.E. Awe, *J. Non Cryst. Sol.* **353**, 1167-1171 (2007).

Received: 20 November 2014.